



Glyceraldehyde-derived advanced glycation end-products having pyrrolopyridinium-based crosslinks

Tomoaki Shigeta^{*}, Kazumi Sasamoto, Tetsuro Yamamoto

Bloom Technology Corporation, 3-14-3 Minamikumamoto, Kumamoto, 860-0812, Japan

ARTICLE INFO

Keywords:

Advanced glycation end-product
Glyceraldehyde
Pyrrolopyridinium
Receptor for AGE
Photosensitization
Singlet oxygen

ABSTRACT

Reducing sugars and reactive aldehydes, such as glyceraldehyde, non-enzymatically react with amino or guanidino groups of proteins to form advanced glycation end-products (AGEs) by the Maillard reaction that involves Schiff base formation followed by Amadori rearrangement. AGEs are found relatively in abundance in the human eye and to accumulate at a higher rate in diseases that impair vision such as cataract, diabetic retinopathy or age-related macular degeneration. We identified two novel AGEs of pyrrolopyridinium lysine dimer derived from glyceraldehyde, PPG1 and PPG2, in the Maillard reaction of *N*^ε-acetyl-L-lysine with glyceraldehyde under physiological conditions. Having fluorophores similar to that of vesperlysine A, which was isolated from the human lens, PPGs were found to act as photosensitizers producing singlet oxygen in response to blue light irradiation. Moreover, PPG2 interacts with receptor for AGE (RAGE) *in vitro* with a higher binding affinity than GLAP, a well-known ligand of the receptor. We also proposed a pathway to form PPGs and discussed how they would be formed *in vitro*. As glyceraldehyde-derived AGEs have been studied extensively in connection with various hyperglycemia-related diseases, further studies will be required to find PPGs *in vivo* such as in the lens or other tissues.

1. Introduction

Advanced glycation end-products (AGEs) are produced non-enzymatically by the Maillard reaction typically between amino or guanidino groups of proteins and reducing sugars or sugar-derived reactive aldehydes. Although AGEs are well known to cause food browning, they are also found to accumulate *in vivo* and therefore drawing attention largely from pathogenic points of view. For instance, proteins of the human eye are highly susceptible to the formation of AGEs that accumulate with age in the lens and retina particularly at higher rates in diseases that impair vision such as cataract, diabetic retinopathy and age-related macular degeneration [1,2]. In the lens, AGEs induce irreversible changes in structural proteins to form high-molecular-weight aggregates that scatter light and impede vision. A milestone in the AGE research is the discovery of pentosidine by Sell and Monnier [3], which is a fluorescent protein-crosslink that accumulates in the lens with age [4]. Another fluorescent crosslink with lysine residues, vesperlysine A, was also identified as a specific marker

for a diabetic process in the human lens [5,6]. These discoveries established that AGEs were integral to the lens aging and subsequent cataract formation. Indeed, there are more than 15 AGEs that have been identified to date in the human lens [2].

Fluorescent AGEs tend to generate reactive oxygen species (ROS) when irradiated by ultraviolet A (UVA) light. Previous studies described that pentosidine generated ROS and singlet oxygen in response to UVA irradiation [7,8]. In addition, a human lens fluorophore LM-1, which was found to be identical to vesperlysine A [6], has also been reported to produce singlet oxygen under the same conditions [7]. These reports indicate that UVA-photosensitized AGEs induce ROS-mediated damages to tryptophan and histidine residues in lens proteins. Therefore, photosensitive AGEs, if accumulated in the lens, possibly play a role in the pathogenesis of the diseases of the eye by photosensitization-induced oxidative stress.

Among many AGEs reported thus far, we have focused on glyceraldehyde-derived AGEs (Glycer-AGEs) in this study mainly because pentosidine, one of the most common fluorescent AGEs, was

Abbreviations: Ac-Lys, *N*^ε-acetyl-L-lysine; Ac-Lys(Z), *N*^ε-acetyl-*N*^ε-carbobenzoxy-L-lysine; AGE, advanced glycation end-product; Glycer-AGEs, glyceraldehyde-derived AGEs; DMSO, dimethyl sulfoxide; GLAP, glyceraldehyde-derived pyridinium compound; L-H-T, lys-hydroxy-triosidine; RAGE, receptor for AGE; ROS, reactive oxygen species.

^{*} Corresponding author.

E-mail addresses: tshigeta@bloom-technology.co.jp, k7299110@kadai.jp (T. Shigeta).

<https://doi.org/10.1016/j.bbrep.2021.100963>

Received 16 September 2020; Received in revised form 10 January 2021; Accepted 22 February 2021

2405-5808/© 2021 Published by Elsevier B.V. This is an open access article under the CC BY-NC-ND license (<http://creativecommons.org/licenses/by-nc-nd/4.0/>).

reported to be produced in the Maillard reaction of N^{ϵ} -acetyl-lysine and N^{ϵ} -acetyl-arginine with glyceraldehyde under physiological conditions [9]. In addition, Nakamura et al. identified fluorescent AGEs having a unique pyrrolopyridinium structure, vesperlysines, also in a similar reaction with glyceraldehyde and *n*-pentylamine (Fig. S1) [5]. Glyceraldehyde can be produced *in vivo* most likely from aldolase-catalyzed conversion of fructose 1-phosphate in polyol metabolism, which is facilitated under high glucose conditions [10]. Glycer-AGEs have been suggested to be associated with a variety of diseases related to hyperglycemia [11]. Furthermore, recent evidence suggests that the interaction of Glycer-AGEs with the receptor for AGEs (RAGE) elicits oxidative stress in numerous types of cells, which might contribute to the pathological changes observed in diabetic complications such as diabetic retinopathy [1,12–14]. We therefore suppose that glyceraldehyde can be a key precursor aldehyde to produce AGEs that enhance oxidative stress, particularly in the eye, both in the presence or absence of light. Although glyceraldehyde-derived pyridinium compound (GLAP) and lys-hydroxy-triosidine (L-H-T), which is a pyridinium-type crosslinked AGE, were identified as Glycer-AGEs [15,16], pathogenic roles of Glycer-AGEs still remain elusive.

In this work through extensive mass spectrometry (MS) and nuclear magnetic resonance (NMR) analyses, we have identified two new vesperlysine-like fluorescent AGEs, pyrrolopyridinium lysine dimer derived from glyceraldehyde (PPG1 and PPG2), in which two lysine molecules are crosslinked by pyrrolopyridinium ring structures

(Fig. 1A), as the major products in the Maillard reaction between N^{ϵ} -acetyl-L-lysine and glyceraldehyde. Of these two AGEs, PPG2 was found to be photosensitive to generate singlet oxygen and to have a binding affinity to RAGE. We described herein the structural determination of these AGEs and discussed how they can be formed *in vitro*. In trying to find a new AGE *in vivo* and to explore its pathological roles, *in vitro* approach seems essential to elucidate the chemical structure as well as to further develop an antibody for immunological studies. Although PPGs need to be identified *in vivo*, we think that they might be useful to elucidate pathogenic roles of Glycer-AGEs and to study oxidative stress induced by photosensitization as well as RAGE-mediated signal transduction in the eye.

2. Materials and methods

2.1. Maillard reaction of N^{ϵ} -acetyl-L-lysine with glyceraldehyde

N^{ϵ} -acetyl-L-lysine (Ac-Lys, Tokyo Chemical Industry, Tokyo, Japan) and DL-glyceraldehyde (Nacalai Tesque, Kyoto, Japan) were dissolved at once in 0.5 M phosphate buffer (pH 7.4) at a concentration of 1.0 M each. The resulting solution was sterilized by filtration through a 0.2- μ m filter and then incubated at 37 °C for one week.

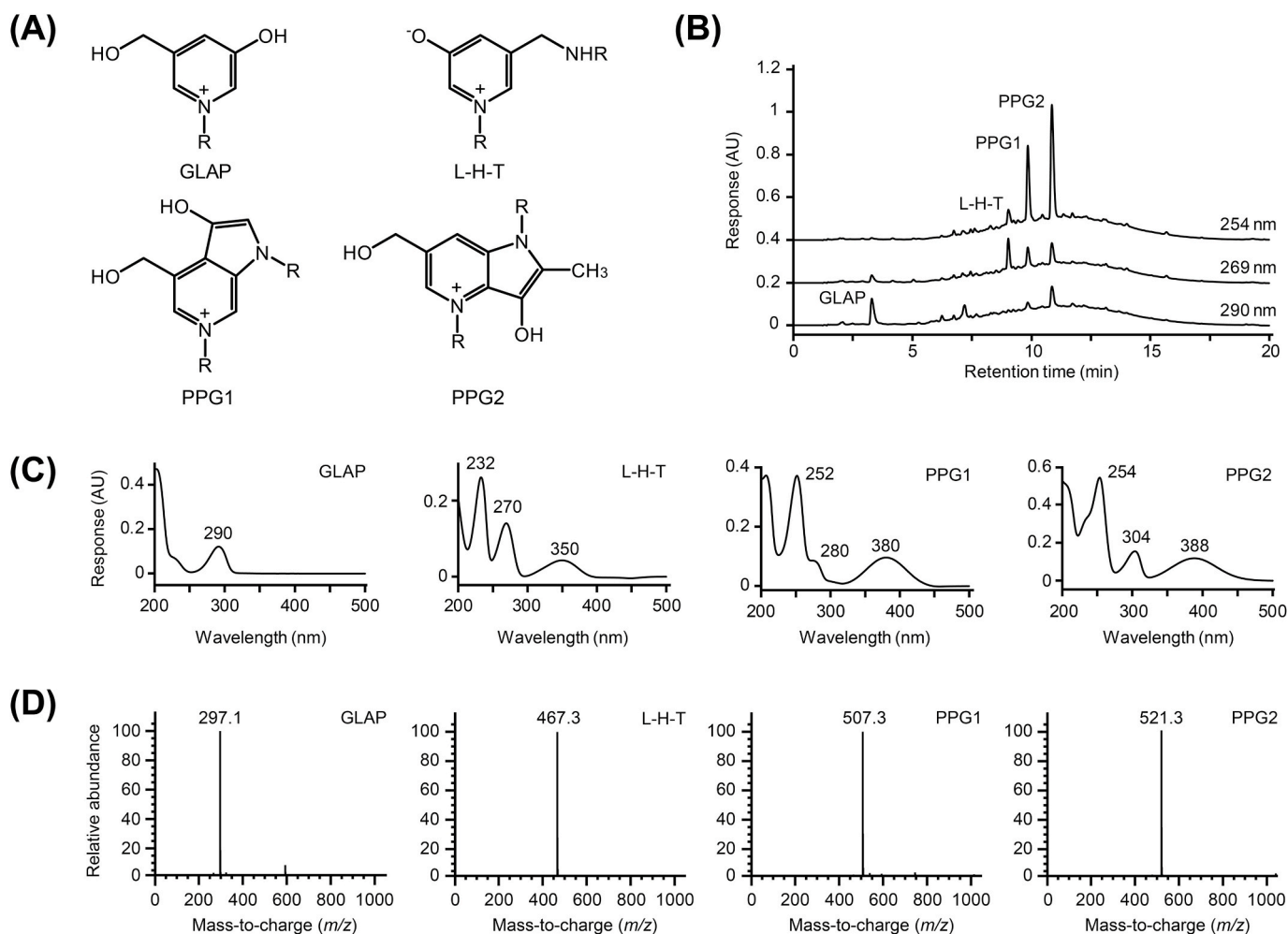


Fig. 1. Detection of GLAP, L-H-T and PPGs in the Maillard reaction mixture of Ac-Lys with glyceraldehyde. (A) Chemical structures of four Glycer-AGEs. R indicates the Ac-Lys moiety. (B) UV chromatograms of the reaction mixture. (C) UV absorbance and (D) single MS spectra of four peaks detected in the Maillard reaction mixture. Detailed analytical conditions are summarized in Table S1.

2.2. Chromatographic purification of the maillard reaction products

The Maillard reaction mixture containing Ac-Lys and glyceraldehyde was subjected to high-performance liquid chromatography (HPLC) equipped with a diode array detector (DAD) and a mass selective detector (MSD) using an Agilent 1260 Infinity II LC/MSD system (Agilent Technologies, Santa Clara, CA, USA). The instrumentation is detailed in our previous report [22]. Chromatographic conditions are summarized in Table S1. Isolation of GLAP, L-H-T and PPGs was performed by a semi-preparative high-performance liquid chromatography (HPLC) with UV signal-triggered fraction collection; the conditions are described in Table S2. Collected fractions were evaporated *in vacuo* and lyophilized to give the product as formate salt.

2.3. Structural determination of PPGs

The chemical composition of PPGs was analyzed using an Agilent 6520 Accurate-Mass Quadrupole Time-of-Flight (Q-TOF) LC/MS system (Agilent Technologies). The instrumentation is detailed in our previous report [22]. Analytical conditions are summarized in Tables S3 and S4. The structural assignment of PPGs dissolved in deuterium oxide (D₂O) or dimethyl sulfoxide (DMSO)-d₆ was performed using an AVANCE III HD 500 MHz NMR spectrometer equipped with a QCI CryoProbe at 298 K and the TopSpin pl3.6 software (Bruker, Billerica, MA, USA).

2.4. Assay of Glycer-AGEs binding to RAGE

The CircuLex AGE-RAGE *in vitro* Binding Assay Kit (Medical & Biological Laboratories, Nagoya, Japan) containing a recombinant soluble RAGE and Glycer-AGEs-bovine serum albumin (BSA) was used following the manufacturer's manual. N^ε-acetylated forms of GLAP, L-H-T, and PPGs were used as competitors. Each competitor was dissolved in 50 mM Tris-HCl (pH 8.0) at a concentration of 200 mM and diluted with the kit's Reaction Buffer at final concentrations of 0.5–10 mM. Fifty millimolar of Tris-HCl at pH 8.0 was used as a vehicle control. Absorbance at 450 nm was measured using a Cytation 5 Multi-Mode Reader with the Gen5 software (BioTek Instruments, Winooski, VT, USA).

2.5. Determination of singlet oxygen produced by photosensitization of AGEs

Singlet oxygen photogenerated from Glycer-AGEs was measured using an electron spin resonance (ESR) spectrometer with a sterically hindered amine according to the literature [17]. A procedure of sample preparation is summarized in Table S5. Briefly, the sample was mixed with 4-hydroxy-2,2,6,6-tetramethylpiperidine (4-OH-TEMPO, Tokyo Chemical Industry) in 0.2 M phosphate buffer (pH 7.5) and the solution was irradiated for 30 min under blue light with illuminance of approximately 1500 lux by a handy LED flashlight with a wavelength of 470 nm (MeCan Imaging, Saitama, Japan). As an authentic singlet oxygen quencher, astaxanthin (FUJIFILM Wako Pure Chemical, Osaka, Japan) was used as a DMSO solution. After the irradiation, ESR spectrum of the sample was recorded on an ELEXSYS-II E580 X-band ESR spectrometer (Bruker) to detect 4-hydroxy-2,2,6,6-tetramethylpiperidine-1-oxyl (4-OH-TEMPO) radical. Instrumental parameters are summarized in Table S6. Spectral simulations were performed using the Xepr software with SpinFit and SpinCount modules (Bruker).

3. Results and discussion

3.1. HPLC analysis of the maillard reaction mixture of Ac-Lys and glyceraldehyde

Ac-Lys was incubated with an equimolar amount of glyceraldehyde under physiological conditions, and the reaction mixture was analyzed by a reversed-phase HPLC equipped with a DAD and a MSD. When

detected at 290 nm, the most intense peak appeared at the retention time (R_t) of 3.3 min, whose absorption maximum was 290 nm (Fig. 1B and C). The MS spectrum of this peak corresponded to that of GLAP as a positive ion with mass-to-charge (*m/z*) of 297 (Fig. 1D). After semi-preparative purification of this peak by HPLC with UV detection as shown in Fig. S2, the chemical structure was confirmed to be GLAP using several NMR techniques, the data of which were identical to those reported previously [15] (Figs. S3–S5). In a similar manner, the peak detected at 269 nm and R_t of 9.0 min (Fig. 1B) was next isolated and its chemical structure was determined to be L-H-T based on the UV–visible spectrum (Fig. 1C), MS spectrum (Fig. 1D) and NMR spectra (Figs. S6–S8). Surprisingly, when detected with a DAD at 254 nm, two intense peaks appeared at R_t of 9.9 min and 10.9 min corresponding to PPG1 and PPG2, respectively (Fig. 1B). The UV–visible spectra indicated the absorption maxima at 252 nm, 280 nm and 380 nm for PPG1 and 254 nm, 304 nm and 388 nm for PPG2, respectively (Fig. 1C). The absorption maxima of PPGs at longer wavelengths compared to those of GLAP and L-H-T suggest that PPGs have an aromatic moiety different from pyridinium structures of GLAP or L-H-T. The single quadrupole MS spectra of PPG1 and PPG2 showed a positive ion at *m/z* 507 and 521, respectively (Fig. 1D), indicating that PPGs are crosslinked dimer analogs of lysine.

3.2. Structural analysis of PPGs

For the subsequent structural analysis, PPGs were isolated by a semi-preparative HPLC (Fig. S2), by which we collected 3.1 mg (5.6 μmole) of PPG1 and 5.4 mg (9.5 μmole) of PPG2 (both as formate) per 1 mL of the Maillard reaction mixture. GLAP and L-H-T were also collected to afford 1.6 mg (4.9 μmole) and 2.2 mg (4.5 μmole), respectively, per 1 mL of the same reaction mixture. The purified PPGs were then subjected to accurate mass measurement and product ion scan using a Q-TOF LC/MS instrument. Fig. S9 shows the monoisotopic mass of PPG1 as an ion at *m/z* 507.2444 in the positive ion mode, which was estimated to be C₂₄H₃₅N₄O₈⁺ (calculated mass 507.2449). The monoisotopic mass of another peak, PPG2, was observed as an ion at *m/z* 521.2603 in the positive ion mode (Fig. S9), which was estimated to be C₂₅H₃₇N₄O₈⁺ (calculated mass 521.2606). In fragmentation analysis of PPGs, the tandem MS (MS/MS) spectra of PPG1 and PPG2 showed a common fragment ion at *m/z* 84.0816 and *m/z* 84.0812, respectively (Fig. S9). Since the positive ion at *m/z* 84 was reported to be a specific MS/MS fragment ion of glycated lysine products observed in LC-MS/MS analysis [18], the fragment ion of PPGs at *m/z* 84 was assigned to be 2,3,4,5-tetrahydropyridinium ion derived from deacetylated Ac-Lys (Fig. S9). From these Q-TOF LC/MS analyses, PPG1 and PPG2 were characterized to have the crosslinking core structures whose molecular formulae are C₈H₇N₂O₂⁺ and C₉H₉N₂O₂⁺, respectively.

To elucidate these crosslinking structures, we next performed several NMR experiments. The data of PPG1 including ¹H, ¹³C, COSY, NOESY, ¹H-¹³C edited-HSQC, 1,1-ADEQUATE and ¹H-¹³C/¹⁵N HMBC are summarized in Fig. S10. ¹H- and ¹³C-NMR spectra indicated that PPG1 has 3 aromatic protons appeared as singlets between 7.7–9.0 ppm and 7 aromatic carbons between 125–139 ppm (Figs. S11 and S12). Additionally, the spectrum of ¹H-¹⁵N HMBC demonstrated that these aromatic protons correlated with the two nitrogens of different chemical properties (at position 1 and 4 in Fig. S13). The aromatic ring of PPG1 was suggested from these ¹H-¹⁵N HMBC and MS/MS spectra (Figs. S9 and S13) to contain both tertiary and quaternary nitrogens. PPG1 was finally identified to be: 1,4-disubstituted 6-hydroxy-8-(hydroxymethyl)-1H-pyrrolo[5,6-c]pyridin-1-ium, as shown in Fig. S10.

The structural determination of PPG2 was achieved in the same manner as PPG1, and the NMR results obtained are summarized in Fig. S14. ¹H- and ¹³C-NMR spectra indicated that PPG2 has 2 aromatic protons between 8.3–8.4 ppm appeared as two singlets and 7 aromatic carbons between 125–144 ppm (Figs. S15 and S16). In the ¹H-NMR spectrum of PPG2, a singlet peak appeared at 2.5 ppm was distinctive

compared to PPG1, which was assigned to the methyl group conjugated to the pyrrole ring (Figs. S14 and S15). The $^1\text{H-NMR}$ spectrum measured in D_2O showed a peak of the methylene protons almost overlapped with that of residual water at 4.8 ppm (Fig. S15), but when measured in DMSO-d_6 , the methylene protons were observed as a singlet with improved resolution between 4.6–5 ppm (Fig. S19). The NMR data of PPG2 in DMSO-d_6 are summarized in Fig. S18; $^1\text{H-}$ and $^{13}\text{C-NMR}$ spectra in DMSO-d_6 are shown in Figs. S19 and S20, respectively. The spectrum of $^1\text{H-}^{15}\text{N}$ HMBC demonstrated that the aromatic protons of PPG2 correlated with the two nitrogens of different chemical properties (at position 1 and 5 in Fig. S17). Like PPG1, the aromatic ring of PPG2 was thought to contain both quaternary and tertiary nitrogens from the $^1\text{H-}^{15}\text{N}$ HMBC as well as MS/MS spectral data (Figs. S9 and S17). These NMR data characterized PPG2 to have the following structure: 1,4-disubstituted 3-hydroxy-8-(hydroxymethyl)-4-methyl-1*H*-pyrrolo[3,4-*b*]pyridin-1-ium, as shown in Fig. S14. To further confirm this aromatic core structure, $^{13}\text{C-}^{13}\text{C}$ INADEQUATE experiment was carried out to observe the carbon-carbon correlation (Fig. S21). The spectral data also supported the interesting carbon skeleton in which the positional relationship of the two nitrogens in the pyrrolopyridinium ring is different from that of PPG1.

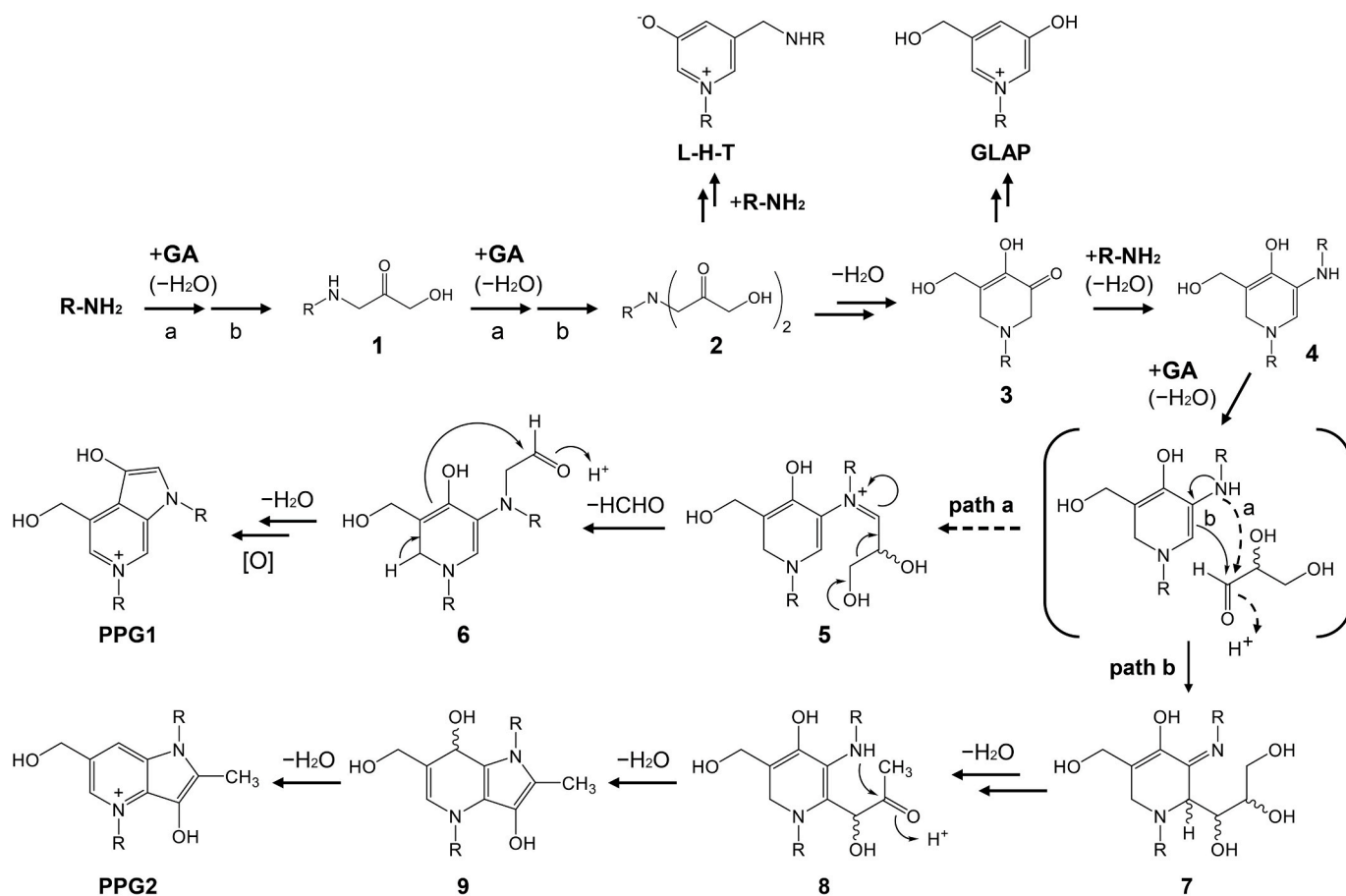
Similar pyrrolopyridinium structures were first reported as vesperlysines in the Maillard reaction of lysine with glucose [5]. However, as discussed by Tessier et al. who isolated vesperlysine A from the human lens proteins [6], the precursor aldehyde and the mechanism to produce vesperlysine A have remained unclear. As Nakamura et al. pointed out that vesperlysines were produced from one of glycoxidation products of glucose [5], we suppose that glyceraldehyde is an important precursor aldehyde to form the AGEs having pyrrolopyridinium

structures.

3.3. Putative pathway to form PPGs in the maillard reaction of Ac-Lys with glyceraldehyde

Scheme 1 illustrates our proposed pathway to produce both PPG1 and PPG2. The initial Maillard reaction to expand the skeleton involves Schiff base formation between the ϵ -amino group of lysine and glyceraldehyde followed by Amadori rearrangement, resulting in the formation of adduct 2. By being dehydrated, adduct 2 cyclizes to give intermediate 3, a common precursor to GLAP as well. Although less likely, intermediate 3 can be further crosslinked to another lysine molecule via its keto functionality to give intermediate 4, which is further coupled with glyceraldehyde in two different mechanisms, as shown in path a and path b in Scheme 1. In path a which involves Schiff base formation, product 5 loses formaldehyde to give aldehyde 6, instead of Amadori rearrangements. The loss of formaldehyde is more likely in this case since it is also supposed in the formation mechanism of pentosidine [9]. Further spontaneous cyclization of aldehyde 6, followed by two-electron oxidation, finally affords PPG1. In contrast to path a, path b involves an aldol-type coupling reaction with glyceraldehyde to form the C-C bond, instead of C-N bond formation in Schiff base formation, yielding adduct 7. It seems unique that the direct C-C bond formation takes place to expand the skeleton in these steps. Adduct 7 is dehydrated to give ketone 8, which facilitates the intramolecular pyrrole ring formation yielding 9. Further dehydration of 9 finally affords PPG2.

As described above, Nakamura et al. reported the formation of AGEs of the same pyrrolopyridinium structures but with different substitution



Scheme 1. A proposed pathway that produces PPGs in the Maillard reaction between glyceraldehyde (GA) and N^α -acetyl-L-lysine (R-NH_2). Reaction conditions: a, Schiff base formation; b, Amadori rearrangement; [O], oxidation.

patterns (vesperlysines, Fig. S1) in the Maillard reaction with *n*-pentylamine and glyceraldehyde, but they did not discuss how vesperlysines were produced in terms of reaction mechanism [5]. Although they performed the instrumental analysis of vesperlysines using fully acetylated derivatives, which differs slightly from our method, the reason that their similar reaction produced different molecules from PPGs is currently unclear.

Similarly, GLAP was also reported by Usui et al. to be the major product in the Maillard reaction with the same substrates as those that we used in our work, Ac-Lys and glyceraldehyde [15]. They carried out the reaction, however, under conditions with much lower substrate concentrations (0.1 M and 0.2 M for Ac-Lys and glyceraldehyde, respectively). Under the identical conditions to those used by Usui et al., the PPG peaks were not observed in a reversed-phase HPLC analysis equipped with a DAD (data not shown), suggesting that the formation of PPGs depends on a ratio of Ac-Lys to glyceraldehyde. In Scheme 1, GLAP is produced via intermediate 3, where, in the case of PPGs, intermediate 3 undergoes further Schiff base formation with Ac-Lys to produce intermediate 4. Our reaction conditions using equimolar amounts of Ac-Lys and glyceraldehyde might facilitate the intermolecular rather than intramolecular reaction to produce 4, instead of GLAP, in a concentration-dependent manner. Probably because of a huge chemical space of the Maillard reaction, the reaction is thought to give a variety of products depending on the reaction conditions, which gives us a basis to believe that PPGs have a chance to be found *in vivo*.

3.4. *In vitro* interaction of PPGs with RAGE

To investigate whether PPGs bind to RAGE, we evaluated *in vitro* inhibitory capacity of PPGs in the binding of a recombinant soluble RAGE with Glycer-AGEs-BSA, a well-known RAGE-binding AGE. The inhibitory capacity in the assay system means the binding capacity of PPGs to RAGE. Since quartz crystal microbalance analyses revealed that *N*^α-acetylated form of GLAP bound to RAGE in a dose-dependent manner [23], we used *N*^α-acetyl-GLAP as a positive control in the RAGE-AGE interaction and evaluated the binding capacity of *N*^α-acetyl-PPGs and L-H-T to RAGE. As shown in Fig. 2, GLAP inhibited the binding between RAGE and Glycer-AGEs-BSA more than 40 % at a concentration of 6 mM compared to the vehicle sample. PPG2 similarly inhibited the binding more than 40 % at a concentration of 4 mM, suggesting that PPG2 is a ligand for RAGE with a higher binding affinity than GLAP. PPG1 and L-H-T, in contrast, were found to show a weak binding inhibition toward RAGE. The 3-hydroxypyridinium structure of GLAP was previously described by Murakami et al. to be essential as the binding moiety in the interaction with RAGE [19]. Our results, however, suggest that a pyridinium ring substituted at its *meta* position with a hydroxymethyl

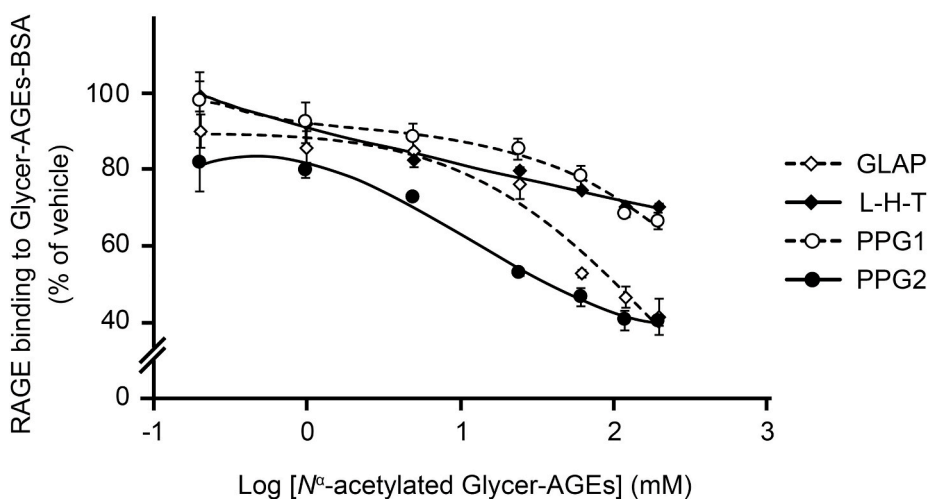


Fig. 2. Binding inhibition of RAGE and Glycer-AGEs-BSA by *N*^α-acetylated Glycer-AGEs *in vitro*. Purified four Glycer-AGEs were used as competitors in the binding assay of His-tagged soluble RAGE with Glycer-AGEs-BSA. Relative RAGE and Glycer-AGEs-BSA binding rate is calculated as relative absorbance at 450 nm in the presence of each competitor against its vehicle control and represented as an average of two independent experiments with standard derivatives. The concentration of competitors used (0.5, 1, 2, 4, 6, 8 and 10 mM) is represented as logarithm. Dose response curve is represented as a third order polynomial curve.

group, which both GLAP and PPG2 have in common, would be important in binding to RAGE rather than a 3-hydroxypyridinium structure. It is also interesting that, despite being a crosslinked type of AGE, PPG2 can interact with RAGE.

As mature AGEs such as pentosidine and vesperlysines are formed over the years as chemical modifications on the ε-amino or guanidino group of lysine or arginine residue, respectively, of long-life proteins, we used Ac-Lys, which is *N*^α-acetylated, as a model of such modification to block the reactions of the α-amino group. In fact, the same reaction with non-acetylated lysine gave very complex reaction mixture that seemed almost impossible to isolate any single molecules. Although we think it unlikely that PPGs in the form of amino acids (not proteins) exist *in vivo*, further studies will be needed to consider the effect of the *N*^α-acetyl group as well as to prove that non-acetylated PPG2 is also a ligand for RAGE. Deprotecting acetylated PPGs using a similar approach employed for *N*^α-acetylated GLAP and L-H-T, in which deprotection was performed by acid hydrolysis, might be an option [16,19].

As GLAP was also suggested by Matsui et al. to be a main structure of Glycer-AGEs that increased ROS production and upregulated inflammatory and thrombogenic gene expression in human umbilical vein endothelial cells via its binding to RAGE [23], it is interesting to know whether PPGs, particularly PPG2 if it exists *in vivo*, have similar biological activities to GLAP such as stimulating RAGE-regulated oxidative and inflammatory reactions.

3.5. Photosensitization of PPGs

Both PPG1 and PPG2 are fluorescent with their emission maxima at 450 nm when excited at their excitation maxima at 350 nm and 380 nm for PPG1 and PPG2, respectively, at pH 7.5 (Fig. S22). Since the fluorescence properties of PPGs are similar to those of vesperlysine A that fluoresces at 442 nm (excited at its excitation maximum at 366–383 nm) [5], PPGs were also expected to exhibit photosensitization effects due to their pyrrolopyridinium structures. We tried to detect singlet oxygen generated from PPGs by light irradiation using an ESR spectrometer. A short-wavelength visible blue light (wavelength at 470 nm) was used to photosensitize PPGs because blue light can be more phototoxic to the eye. For example, blue light was reported to induce apoptosis of rat retinal cells [20]. In the ESR experiment, singlet oxygen was measured quantitatively as an amount of 4-OH-TEMPO radical, a stable nitroxide radical, that is produced by the reaction of 4-OH-TEMP with singlet oxygen, as shown in Fig. 3, in which black columns indicate that the samples were not irradiated (placed in dark). All AGEs were observed to generate singlet oxygen compared to Ac-Lys(Z), a fully protected lysine analog as a negative control. The ESR signals of these AGEs decreased by the presence of astaxanthin, a specific quencher of singlet oxygen [21],

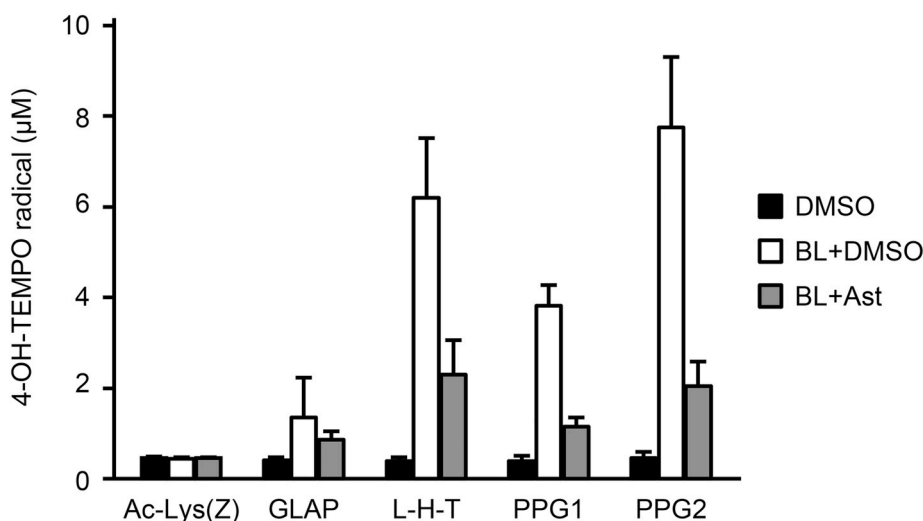


Fig. 3. Effects of photosensitization of purified Glycer-AGEs shown as the relative yield of singlet oxygen. Ac-Lys(Z) and purified four Glycer-AGEs (2.5 mM each) were reacted with 4-OH-TEMPO (100 mM) with or without blue light (BL) irradiation for 30 min, in the presence of astaxanthin (Ast, 5 mM) or DMSO as a vehicle control. ESR measurements were performed to detect 4-OH-TEMPO radical ($g = 2.0057$) produced from the oxidation of 4-OH-TEMPO by singlet oxygen. The spectra consisting of three lines with isotropic ^{14}N -hyperfine splitting constants of 16.86 G (1 N) was used to determine a spin concentration of 4-OH-TEMPO by the Xepr software. The data are represented as an average of three independent measurements with standard derivatives.

which further supports the generation of singlet oxygen induced by photosensitization. All crosslinked-type AGEs (PPGs and L-H-T) showed substantial photosensitization effects, whereas non-crosslinked type AGE (GLAP) was found to generate a much smaller amount of singlet oxygen under identical conditions probably because of lack of long-wavelength light absorptions (Fig. 1C).

In summary, AGEs tend to accumulate particularly in the eye which is constantly exposed to light [2]. Photosensitive AGEs, if accumulated in the eye, could enhance oxidative stress and causes various damages of the eye. Glyceraldehyde has been suggested to be a precursor aldehyde to form fluorescent AGEs, such as pentosidine and vesperlysines, both of which are photosensitive as well [5–9]. Also, Glycer-AGEs were suggested to play roles in various hyperglycemia-related diseases [11]. We have identified in this work novel Glycer-AGEs, PPG1 and PPG2, in which two lysine molecules are crosslinked via the pyrrolopyridinium ring structures, in the Maillard reaction between Ac-Lys and glyceraldehyde under physiological conditions. Both PPGs are photosensitive to generate singlet oxygen by light irradiation, and PPG2 shows a binding affinity toward RAGE. We have also proposed a mechanism, by which both PPGs are formed *in vitro*, and which involves a unique skeleton expansion reaction in addition to the typical Schiff base formation.

In order to find PPGs *in vivo*, it is important to know the acid stability of PPGs because it requires an acid hydrolysis of tissue samples and also helps to find conditions to deprotect acetylated PPGs. Since Nakamura et al. reported that vesperlysines were stable to acid hydrolysis [5], we expect that PPGs are also stable to these acidic conditions. As an alternative approach to identify PPGs in cells and tissues, we also plan to perform immunohistochemical studies by developing monoclonal antibodies against PPGs. Although further study is required to detect PPGs *in vivo*, we expect future applications of PPGs as useful tools in the AGE research, in particular, to investigate pathogenic aspects of Glycer-AGEs that induce oxidative stress by photosensitization as well as RAGE-mediated signal transduction in the eye.

Funding sources

We have not received any specific grant from funding agencies in the public, commercial or non-profit sectors for this research.

Credit author statement

Tomoaki Shigeta: Conceptualization, Methodology, Validation, Investigation, Data Curation, Writing - Original Draft, Writing - Review & Editing, Project administration. **Kazumi Sasamoto:** Conceptualization, Writing - Original Draft, Writing - Review & Editing, Project

administration, Supervision. **Tetsuro Yamamoto:** Writing - Review & Editing, Supervision.

Declaration of competing interest

The authors declare that they have no known competing financial interests or personal relationships that could have appeared to influence the work reported in this paper.

Acknowledgements

We appreciate Professor Masayoshi Takeuchi of Kanazawa Medical University for providing helpful information in AGE research. We are grateful to Professors Naomi Nakagata and Toru Takeo of Kumamoto University for their assistance in this study. We appreciate Drs. Teppei Kanaba and Hideyuki Hara of Bruker Japan for technical advice in the NMR and ESR analysis. We used the NMR and ESR instruments in Core Laboratory for Medical Research and Education, School of Medicine, Kumamoto University. We also appreciate Dr. Takao Sato of Kumamoto Industrial Research Institute for technical advice in the analysis with Q-TOF LC/MS which is owned by Kumamoto Industrial Research Institute. We thank Keiko Hayashi of Agilent Technologies for technical advice in peak-based fraction collection.

Appendix A. Supplementary data

Supplementary data to this article can be found online at <https://doi.org/10.1016/j.bbrep.2021.100963>.

References

- [1] H. Zong, M. Ward, A.W. Stitt, AGEs, RAGE, and diabetic retinopathy, *Curr. Diabetes Rep.* 11 (2011) 244–252, <https://doi.org/10.1007/s11892-011-0198-7>.
- [2] R.H. Nagaraj, M. Linetsky, A.W. Stitt, The pathogenic role of Maillard reaction in the aging eye, *Amino Acids* 42 (2012) 1205–1220, <https://doi.org/10.1007/s00726-010-0778-x>.
- [3] D.R. Sell, V.M. Monnier, Structure elucidation of a senescence cross-link from human extracellular matrix. Implication of pentoses in the aging process, *J. Biol. Chem.* 264 (1989) 21597–21602, [https://doi.org/10.1016/S0021-9258\(20\)88225-8](https://doi.org/10.1016/S0021-9258(20)88225-8).
- [4] R.H. Nagaraj, D.R. Sell, M. Prabhakaram, B.J. Ortwerth, V.M. Monnier, High correlation between pentosidine protein crosslinks and pigmentation implicates ascorbate oxidation in human lens senescence and cataractogenesis, *Proc. Natl. Acad. Sci. Unit. States Am.* 88 (1991) 10257–10261, <https://doi.org/10.1073/pnas.88.22.10257>.
- [5] K. Nakamura, Y. Nakazawa, K. Ienaga, Acid-stable fluorescent advanced glycation end products: vesperlysines A, B, and C are formed as crosslinked products in the maillard reaction between lysine or proteins with glucose, *Biochem. Biophys. Res. Commun.* 232 (1997) 227–230, <https://doi.org/10.1006/bbrc.1997.6262>.

- [6] F. Tessier, M. Obrenovich, V.M. Monnier, Structure and mechanism of formation of human lens fluorophore LM-1, *J. Biol. Chem.* 274 (1999) 20796–20804, <https://doi.org/10.1074/jbc.274.30.20796>.
- [7] B.J. Ortwerth, M. Prabhakaram, R.H. Nagaraj, M. Linetsky, The relative UV sensitizer activity of purified advanced glycation endproducts, *Photochem. Photobiol.* 65 (1997) 666–672, <https://doi.org/10.1111/j.1751-1097.1997.tb01909.x>.
- [8] Y. Okano, H. Masaki, H. Sakurai, Pentosidine in advanced glycation end-products (AGEs) during UVA irradiation generates active oxygen species and impairs human dermal fibroblasts, *J. Dermatol. Sci.* 27 (2001) 11–18, [https://doi.org/10.1016/s0923-1811\(01\)00114-1](https://doi.org/10.1016/s0923-1811(01)00114-1).
- [9] P. Chellan, R.H. Nagaraj, Early glycation products produce pentosidine cross-links on native proteins. Novel mechanism of pentosidine formation and propagation of glycation, *J. Biol. Chem.* 276 (2001) 3895–3903, <https://doi.org/10.1074/jbc.M008626200>.
- [10] C.G. Schalkwijk, C.D.A. Stehouwer, V.W.M. van Hinsbergh, Fructose-mediated non-enzymatic glycation: sweet coupling or bad modification, *Diabetes Metab. Res. Rev.* 20 (2004) 369–382, <https://doi.org/10.1002/dmrr.488>.
- [11] M. Takeuchi, S. Yamagishi, TAGE (toxic AGEs) hypothesis in various chronic diseases, *Med. Hypotheses* 63 (2004) 449–452, <https://doi.org/10.1016/j.mehy.2004.02.042>.
- [12] M. Takeuchi, J. Takino, S. Yamagishi, Involvement of TAGE-RAGE system in the pathogenesis of diabetic retinopathy, *J. Ophthalmol.* 2010 (2010) 1–12, <https://doi.org/10.1155/2010/170393>.
- [13] T. Sato, M. Iwaki, N. Shimogaito, X. Wu, S. Yamagishi, M. Takeuchi, TAGE (toxic AGEs) theory in diabetic complications, *Curr. Mol. Med.* 6 (2006) 351–358, <https://doi.org/10.2174/156652406776894536>.
- [14] Y. Yamamoto, H. Yonekura, T. Watanabe, S. Sakurai, H. Li, A. Harashima, K. M. Myint, M. Osawa, A. Takeuchi, M. Takeuchi, H. Yamamoto, Short-chain aldehyde-derived ligands for RAGE and their actions on endothelial cells, *Diabetes Res. Clin. Pract.* 77 (2007) S30–S40, <https://doi.org/10.1016/j.diabres.2007.01.030>.
- [15] T. Usui, F. Hayase, Isolation and identification of the 3-hydroxy-5-hydroxymethylpyridinium compound as a novel advanced glycation end product on glyceraldehyde-related Maillard reaction, *Biosci. Biotechnol. Biochem.* 67 (2003) 930–932, <https://doi.org/10.1271/bbb.67.930>.
- [16] F.J. Tessier, V.M. Monnier, L.M. Sayre, J.A. Kornfield, Triosidines: novel Maillard reaction products and cross-links from the reaction of triose sugars with lysine and arginine residues, *Biochem. J.* 369 (2003) 705–719, <https://doi.org/10.1042/BJ20020668>.
- [17] K. Nakamura, K. Ishiyama, H. Ikai, T. Kanno, K. Sasaki, Y. Niwano, M. Kohno, Reevaluation of analytical methods for photogenerated singlet oxygen, *J. Clin. Biochem. Nutr.* 49 (2011) 87–95, <https://doi.org/10.3164/jcbs.10-125>.
- [18] O.K. Argirov, N.D. Leigh, B.J. Ortwerth, Specific MS/MS fragmentation of lysine, arginine, and ornithine glycation products provides an opportunity for their selective detection in protein acid hydrolysates and enzymatic digests, *Ann. N. Y. Acad. Sci.* 1043 (2005) 903, <https://doi.org/10.1196/annals.1333.117>.
- [19] Y. Murakami, T. Fujino, T. Hasegawa, R. Kurachi, A. Miura, T. Daikoh, T. Usui, F. Hayase, H. Watanabe, Receptor for advanced glycation end products (RAGE)-mediated cytotoxicity of 3-hydroxypyridinium derivatives, *Biosci. Biotechnol. Biochem.* 82 (2018) 312–319, <https://doi.org/10.1080/09168451.2017.1422971>.
- [20] J. Wu, S. Seregard, B. Spångberg, M. Oskarsson, E. Chen, Blue light induced apoptosis in rat retina, *Eye* 13 (1999) 577–583, <https://doi.org/10.1038/eye.1999.142>.
- [21] A.L. Petrou, P.L. Petrou, T. Ntanos, A. Liapis, A possible role for singlet oxygen in the degradation of various antioxidants. A meta-analysis and review of literature data, *Antioxidants* 7 (2018) 1–32, <https://doi.org/10.3390/antiox7030035>.
- [22] T. Shigeta, K. Sasamoto, T. Yamamoto, A novel crosslinked type of advanced glycation end-product derived from lactaldehyde, *Heliyon* 6 (2020), e05337, <https://doi.org/10.1016/j.heliyon.2020.e05337>.
- [23] T. Matsui, E. Oda, Y. Higashimoto, S. ichi Yamagishi, Glyceraldehyde-derived pyridinium (GLAP) evokes oxidative stress and inflammatory and thrombogenic reactions in endothelial cells via the interaction with RAGE, *Cardiovasc. Diabetol.* 14 (2015) 1–10, <https://doi.org/10.1186/s12933-014-0162-3>.